tripotassium citrate, 43.4 mM citric acid, and 10 mM dithiothreitol). Spores and insoluble material were spun out at 8000 rpm. Toxin was precipitated from the supernatant by adding 0.75 ml of 1 M tripotassium citrate and stored at −80°C. Toxin was solubilized by resuspending in 20 mM Hepes (pH 8.0) at a final concentration of 4 mg/ml. To test the quality of this purified toxin, we determined the concentration at which 50% of the animals die after exposure for 5 days at 20°C (LC_{50}) to be 16.7 μg/ml, similar to the 12.6 μg/ml reported for toxin present in crude spore lysates (*6*). Toxin was labeled in the presence of a fourfold molar excess of *N*-hydroxysuccinimide–rhodamine (Pierce 46102) and purified away from unincorporated rhodamine by gel filtration. Labeled toxin has potent but reduced toxicity (LC_{50} = 31.8 μg/ml). Feeding assays were performed with L4-staged hermaphrodites in wells containing egg salts with 100 mM glucose and labeled toxin (50 μg/ml), FM4-64 (20 μg/ml), or rhodamine-BSA (0.1 mg/ml). Images were collected on an Olympus IX-70 inverted microscope (40×, 1.35 NA objective) and a MicroMax camera (Roper Instruments).

23. M. Kostich, A. Fire, D. M. Fambrough, *J. Cell Sci.* **113**, 2595 (2000).
24. J. Payne, K. Narva, World Intellectual Property Organization Patent 94/16079 (1994).
25. _____, J. Fu, U.S. Patent 5,589,382 (1995).
26. As was done previously for Cry5B (*6*), DNA equivalent to the Cry14A coding sequence was cloned into the pQE9 expression vector and transformed into JM103 cells. Single L4-staged hermaphrodites were placed in 120-μl single-well assays that included S medium, antibiotics, and 10 μl of *E. coli* induced to express Cry14A and/or vector alone (*6*). The amount of toxin was quantitated by comparing the Cry14A band against BSA standards on SDS gels and was varied by altering the mixture of bacteria expressing either empty vector or Cry14A. The total optical density of bacteria added to the well was always constant. Brood sizes were counted after 3 days at 25°C. The data from the 19 animals were taken from two independent experiments. We repeated the experiments with *E. coli* expressing Cry5B and found that at a Cry5B concentration of 3.3 μg/ml, wild-type animals had a brood of 5.1 ± 3.3 progeny (n = 20), whereas *bre-5(ye17)* animals had a brood of 99 ± 28 progeny (n = 20, compared to 104 ± 36 progeny without toxin).
27. X. Lee *et al.*, *J. Biol. Chem.* **273**, 6312 (1998).
28. R. Sankaranarayanan *et al.*, *Nature Struct. Biol.* **3**, 596 (1996).

29. We thank L. Marroquin for information that helped in the cloning of *bre-5*, B. Grant for help with endocytosis assays, J. Posakony and B. Oppert for critical reading of the manuscript, J. Esko and members of the Aroian laboratory for helpful discussions, and T. Stiernagle at the *C. elegans* Genetics Center (funded by the NIH National Center for Research Resources) for *C. elegans* stocks. Supported by NSF grant MCB-9983013 (R.V.A.), a Burroughs Wellcome New Investigators Award in Toxicological Sciences, and a Beckman Foundation Young Investigators Award. The GenBank accession number for *bre-5* sequence is AY038065.

10 May 2001; accepted 15 June 2001

Myotonic Dystrophy Type 2 Caused by a CCTG Expansion in Intron 1 of *ZNF9*

Christina L. Liquori,[1,2] Kenneth Ricker,[4] Melinda L. Moseley,[1,2] Jennifer F. Jacobsen,[1,2] Wolfram Kress,[5] Susan L. Naylor,[6] John W. Day,[1,3]* Laura P. W. Ranum[1,2]*

Myotonic dystrophy (DM), the most common form of muscular dystrophy in adults, can be caused by a mutation on either chromosome 19q13 (DM1) or 3q21 (DM2/PROMM). DM1 is caused by a CTG expansion in the 3′ untranslated region of the dystrophia myotonica–protein kinase gene (*DMPK*). Several mechanisms have been invoked to explain how this mutation, which does not alter the protein-coding portion of a gene, causes the specific constellation of clinical features characteristic of DM. We now report that DM2 is caused by a CCTG expansion (mean ~5000 repeats) located in intron 1 of the zinc finger protein 9 (*ZNF9*) gene. Parallels between these mutations indicate that microsatellite expansions in RNA can be pathogenic and cause the multisystemic features of DM1 and DM2.

DM is a dominantly inherited, multisystemic disease with a consistent constellation of seemingly unrelated and rare clinical features including myotonia, muscular dystrophy, cardiac conduction defects, posterior iridescent cataracts, and endocrine disorders (*1*). DM was first described nearly 100 years ago (*2*), but the existence of more than one genetic cause was only recognized after genetic testing became available for myotonic dystrophy type 1 (DM1) (*3, 4*).

DM1 is caused by an expanded CTG repeat on chromosome 19 that is both in the 3′ untranslated region of the dystrophia myotonica–protein kinase (*DMPK*) gene, and in the promoter region of the immediately adjacent homeodomain gene *SIX5* (*5, 6*). How the CTG expansion in a noncoding region of a gene causes the complex DM phenotype remains unclear (*5, 6*). Suggested mechanisms include: (i) haploinsufficiency of the dystrophia myotonica–protein kinase (DMPK) protein (*7*); (ii) altered expression of neighboring genes, including *SIX5* (*8–12*); and (iii) pathogenic effects of the CUG expansion in RNA which accumulates as nuclear foci (*13, 14*) and disrupts cellular function (*15–18*). Several mouse models have developed different aspects of DM1: a model expressing mRNA with CUG repeats manifests myotonia and the myopathic features of DM1 (*19*); a *DMPK* knockout has cardiac abnormalities (*20*); and *SIX5* knockouts have cataracts (*21, 22*). Taken together, these data have been interpreted to suggest that each theory may contribute to DM1 pathogenesis and that DM1 may be a regional gene disorder (*5, 6*).

Defining a second human mutation that causes the multisystemic effects of DM, and identifying what is common to these diseases at the molecular level, provides an independent means of determining the pathogenic pathway of DM. Toward this goal, we mapped the myotonic dystrophy type 2 [DM2/proximal myotonic myopathy (PROMM)] locus to chromosome 3q21 (*23, 24*) and have used positional cloning to identify the DM2 mutation.

The DM2 region was narrowed to a 2-cM interval (*25*) by analyzing 10 recombinant chromosomes (*25*). Sequence data (*26, 27*) from this region, which is partially covered by 14 bacterial artificial chromosomes (BACs), was used to develop 80 short tandem repeat (STR) markers. Linkage disequilibrium analysis (*27*) was performed on 64 parent-offspring trios in which affected individuals had the clinical features of DM but not the DM1 mutation. Transmission disequilibrium testing (*28*) and analysis of conserved ancestral haplotypes narrowed the DM2 locus to a region of ~320 kilobases (kb) (Fig. 1A).

One of the markers in linkage disequilibrium with DM2, *CL3N58* ($P \leq 0.000001$), showed an aberrant segregation pattern. All affected individuals appeared to be homozygous by polymerase chain reaction (PCR) (*29*), and affected children appeared not to inherit an allele from their affected parent (Fig. 1, B and C). Southern (DNA) analysis was performed (*30*) to investigate the possibility that the aberrant segregation pattern was caused by a repeat expansion or other rearrangement. In addition to the expected normal allele, we detected a variably sized expanded allele, too large to amplify by PCR, that was found only in affected individuals (Fig. 1, B and D). Modified electrophoresis conditions

[1]Institute of Human Genetics; [2]Department of Genetics, Cell Biology, and Development; and [3]Department of Neurology MMC 206, 420 Delaware Street SE, University of Minnesota, Minneapolis, MN 55455, USA. [4]Department of Neurology and [5]Institute of Human Genetics, University of Würzburg, Germany. [6]Department of Cellular and Structural Biology, University of Texas Health Science Center at San Antonio, San Antonio, TX 78284, USA.

*To whom correspondence should be addressed. E-mail: johnday@umn.edu (J.W.D.); ranum001@umn.edu (L.P.W.R.).

(*27, 30*) enabled us to resolve a range of expansions between 10 and 48 kb (Fig. 1E).

To determine if this expansion was involved in the DM2 disease process, we performed PCR and Southern analysis on: (i) 51 affected individuals in six families whose disease was consistent with linkage to the DM2 locus; (ii) one affected individual from each of 20 additional families with ancestrally conserved DM2 haplotypes; and (iii) a panel of control genomic samples representing 1360 chromosomes. PCR showed that all 51 affected individuals in the six DM2 families appeared to be homozygous, but each individual had an expanded allele on subsequent Southern analysis (*31*). The maximum lod scores at $\Theta = 0.00$ between the disease locus and the *CL3N58* expansion for the six families were: MN1 = 6.9, MN6 = 1.5, MN10 = 8.2, MN12 = 2.8, F134 = 10.4, and F047 = 1.8. Expanded alleles detected by Southern analysis were also found in affected representatives of all 20 additional families with ancestrally conserved DM2 haplotypes. PCR and Southern analysis identified no control samples with an expansion.

Sequence of the *CL3N58* marker contains the complex repeat motif $(TG)_n(TCTG)_n(CCTG)_n$. In our control group, the size of the $(TG)_n(TCTG)_n(CCTG)_n$ repeat tract ranged from 104 to 176 base pairs (bp) (Heterozygosity = 0.89) (Fig. 2A). All eight normal alleles that were sequenced (*29*) had CCTG repeat tracts that were interrupted by both GCTG and TCTG motifs or by one or two TCTG motifs (Fig. 2B). The repeat tract in the largest normal allele (combined TG/TCTG/CCTG repeats of 176 bp) was sequenced and shown to contain 26 CCTG repeats with two interruptions. Smaller expansions from three DM2 patients were sequenced (*29*), demonstrating that the CCTG portion of the repeat tract is expanded. In contrast to alleles from the control samples, the CCTG repeat tracts on expanded alleles were uninterrupted. Expansion sizes for very large alleles were estimated by Southern analysis assuming that, consistent with the sequenced expansions, lengthening of the CCTG repeat tract accounts for the increase in molecular weight. The range of expanded allele sizes is extremely broad, from 75 to ~11,000 CCTG repeats with a mean of ~5000 (Fig. 2C). Shorter expansions were found in individuals with multiple allele sizes in blood, so that the smallest pathogenic size is uncertain.

In approximately 25% of the affected individuals, we observed two to four bands in DNA isolated from blood, representing expanded alleles of various sizes (Fig. 3A and Web table 1) (*27*). Some bands were discrete in size, some appeared as unresolved compression bands at the top of the gel, and others showed a broad variation of molecular weight. Additional examples of somatic instability included: (i) a pair of genetically confirmed ($P \leq 0.001$) monozygotic twins (31 years old) (*27*) had dramatically different expanded alleles (13 and 24 kb) (Fig. 3B); (ii) the expansion size in lymphocyte DNA from an affected individual increased in size by approximately 2 kb during the 3-year interval between blood donations (Fig. 3C); and (iii) the age of affected individuals at the time they donated a blood sample directly correlated ($r = 0.41$, $r^2 = 0.17$, $P = 0.008$) with the size of the expansion (Fig. 3D). Expansion sizes in the blood of affected children are usually shorter than in their parents: the time-dependent somatic variation of repeat size complicates the interpretation of this difference (Web table 1) (*27*). No significant correlation between age of onset and expansion size was observed.

The DM2 expansion (*CL3N58*) is located in a region of the genome for which the available sequence was not completely ordered. To determine the location of the DM2 expansion, we sequenced portions of the BAC RP11-814L21 to assemble unfinished sequence contigs (*27*). Our sequencing data and sequence from the Human Genome Project (*26*) indicate that the expansion is located in intron 1 of the zinc finger protein 9 (*ZNF9*) gene (Fig. 4A) (*32*), also referred to as the cellular nucleic acid-binding protein gene. ZNF9 contains seven zinc finger domains (*33*) and is thought to be an RNA-binding protein (*34, 35*). Although the originally reported genomic sequence for *ZNF9* (*32, 36*) did not contain the *CL3N58* marker, we have generated additional sequence, used sequence from Celera (*32, 37*) (x2HTBKUAD8C), and performed Southern (*27, 31*) and reverse transcription PCR (RT-PCR) analysis (*31*) to confirm the location of the expansion. *ZNF9* transcripts are broadly expressed and are most abundant in heart and skeletal muscle (Web fig. 1) (*27*), two tissues prominently affected in DM2.

In situ hybridization has been used to detect nuclear foci containing the CUG expansion in DM1 cells (*13*). Because DM2 is also caused by

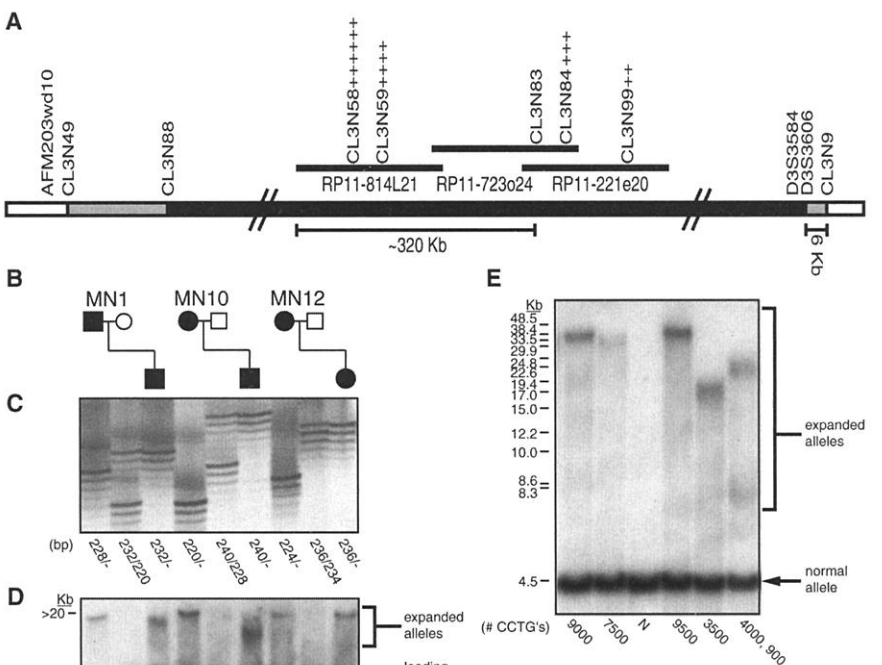

Fig. 1. Expanded *CL3N58* allele found in DM2 patients. (**A**) DM2 critical region. Black represents the minimal DM2 critical region, white represents DM2 excluded regions, and gray represents regions in which recombination has occurred. Markers defining recombination events and establishing linkage disequilibrium are shown, along with previously published markers. The relative significance of the *P*-values are indicated by plusses above the marker names, with "++" ≤ 0.01, "+++" ≤ 0.001 "++++" ≤ 0.0001, and "++++++" ≤ 0.000001. Three BACs (orientation unknown) within the region of linkage disequilibrium are shown. Not drawn to scale. (**B**) Pedigrees of three different DM2-linked families, each represented by a nuclear family. (**C**) PCR analysis of *CL3N58* marker. The genotype of each individual is shown, with each allele given in base pairs. Unamplified alleles are represented by "–". (**D**) Southern-blot analysis of expansion mutations. Individuals with an expanded CCTG track are represented by "EXP," and individuals with two normal alleles are represented by "N." The blot was also hybridized with an SCA8 loading control, showing that all but the first lane was evenly loaded. (**E**) High-resolution sizing of expansions. Lane 3 contains DNA from a control sample. The number of CCTGs of each individual's expanded allele is shown, with "N" representing a normal length CCTG tract.

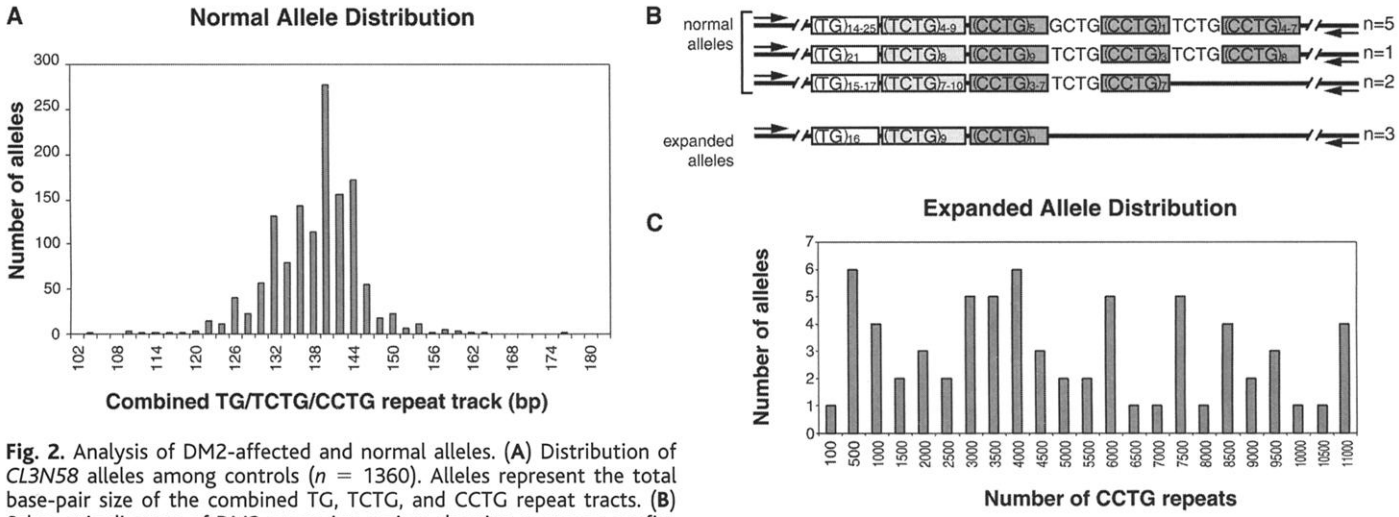

Fig. 2. Analysis of DM2-affected and normal alleles. (**A**) Distribution of *CL3N58* alleles among controls (n = 1360). Alleles represent the total base-pair size of the combined TG, TCTG, and CCTG repeat tracts. (**B**) Schematic diagram of DM2 expansion region, showing sequence configurations of normal and expanded repeat tracts. (**C**) Distribution of expanded alleles among 51 affected members of six DM2 families. All expanded allele sizes were included for individuals with multiple bands and, in contrast to (B), are given in CCTG repeat units.

an expansion motif, we performed fluorescent in situ hybridization (*38*) to determine if similar repeat-containing nuclear foci are found in DM2. Fluorescently labeled antisense oligonucleotide probes to the CCUG repeat were hybridized to control, DM2, and DM1 muscle biopsy tissue. The DM2 muscle biopsy was from an affected member of the 3q-linked MN1 family (LOD = 6.9), who had a CCTG expansion detected by Southern analysis. Similarly, DM1 tissue was taken from a genetically confirmed DM1 patient. Numerous intense CCUG-containing nuclear foci were observed in DM2 (Fig. 4B), but not in control, muscle (Fig. 4C). In DM2 muscle, one to five foci were seen per nucleus, with no foci detected in the cytoplasm. In general, more foci were seen per nucleus in DM2 than were seen using antisense probes to the CUG expansions in DM1 muscle (Fig. 4, B and D). The sense CCUG probes showed no nuclear foci, indicating that the probe hybridized to RNA, not DNA (*31*). Our results show that the CCTG expansion is expressed, but we do not yet know if the RNA foci contain the entire unprocessed ZNF9 transcript. The antisense CCUG probe showed no nuclear foci in DM1 muscle (*31*). Although the antisense probe to the CUG repeat also hybridized to foci in DM2 muscle (*31*), we believe this signal was caused by nonspecific cross-hybridization to the extremely large CCUG repeat tract (11,000 repeats).

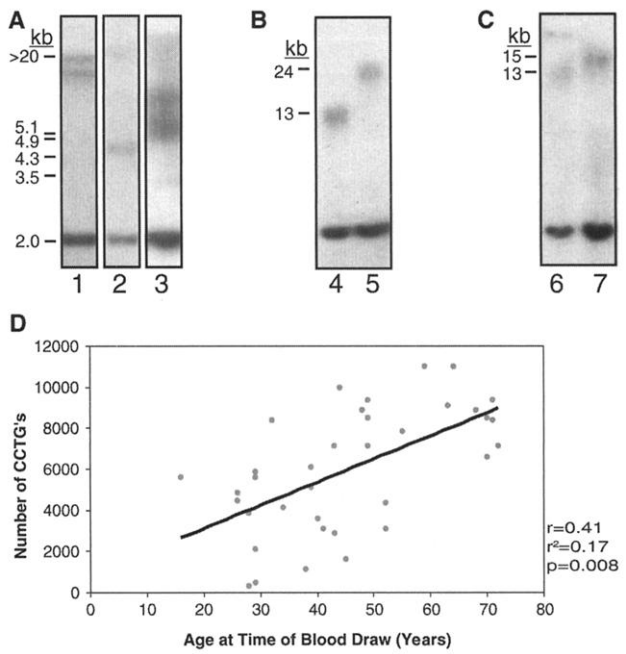

Fig. 3. Instability of the DM2 expansion. (**A**) Somatic heterogeneity in blood. Southern blots of Bso BI–digested genomic DNA from blood revealed multiple expanded alleles in some affected individuals, some discrete in size (lanes 1 and 2) and others broad (lane 3). (**B**) Southern blots of Eco RI–digested genomic DNA from blood of monozygotic twins (lanes 4 and 5). (**C**) Expanded alleles increase in length over time. Southern blot of Eco RI–digested genomic DNA samples from blood taken from a single patient at 28 (lane 6) and 31 (lane 7) years of age, respectively. (**D**) Correlation between the size of the expanded allele in individuals with a single allele and age at the time blood sample was taken.

Our results demonstrate that DM2 is caused by an untranslated CCTG expansion. DM2 shows remarkable clinical similarity to DM1, although the disease course of DM2 is usually more benign. Clinical and molecular parallels between these diseases indicate that the CUG and CCUG expansions expressed at the RNA level can themselves be pathogenic and cause the multisystemic features of DM1 and DM2. The normal function of ZNF9 as an RNA-binding protein (*35, 36*) appears unrelated to any of the proteins encoded in the DM1 region of chromosome 19. Similarly, the genes in the DM2 region (*KIAA1160*, *Rab 11B*, *glycoprotein IX*, *FLJ11631*, and *FLJ12057*) bear no obvious relationship to the genes at the DM1 locus, indicating that the clinical features common to DM1 and DM2 are not related to disruptions in the regulation of genes in the vicinity of these expansions.

Given the similarity of the DM1 and DM2 repeat motifs and the fact that the expansions accumulate as RNA foci, RNA-binding proteins that bind to the DM1 CUG expansion may also bind to the DM2 CCUG expansion, causing similar global disruptions in RNA splicing and cellular metabolism (*15, 17, 18*). One of these proteins has been shown to have a preferential affinity for UG dinucleotides (*39*), which are found in both DM1 and DM2 expansions. If these same RNA-binding proteins are involved in DM2 pathogenesis, then one could speculate that the longer CCUG repeat tracts cause the milder DM2 phenotype because the affinity of these proteins for the CCUG repeat tract is not as strong. Alternatively, a different set of RNA-binding proteins may bind to the CCUG expansion.

DM2 is the fourth example of a dominant disease that is caused by a microsatellite expansion located in a transcribed but untranslated portion of its respective gene. On the molecular level, the CCTG DM2 expansion has parallels to the untranslated CTG expansions involved in both DM1 (*5, 6*) and SCA8 (*40*) as well as the

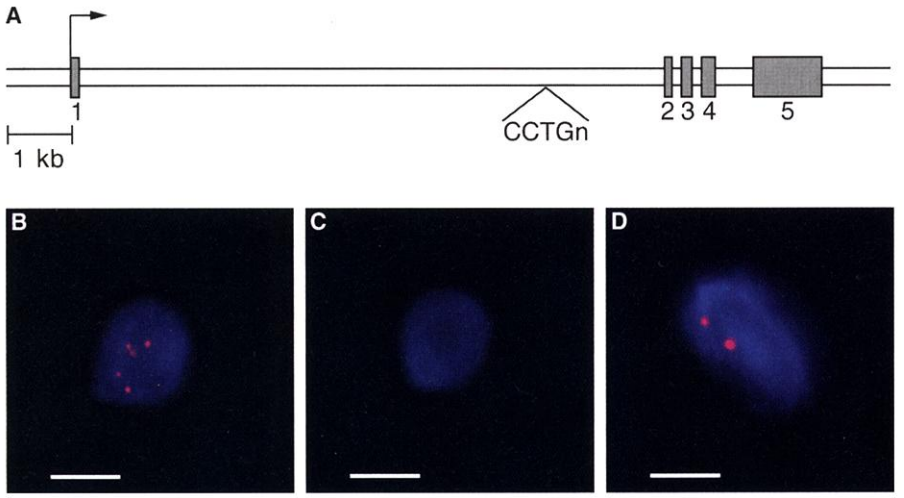

Fig. 4. RNA in situ hybridization of the expansion. **(A)** Genomic organization of the ZNF9 gene. The position of the DM2 expansion in intron 1 is shown. The gene spans 11.3 kb of genomic sequence with an open reading frame of 1.5 kb. **(B)** In situ hybridization of CAGG probe to DM2 muscle. **(C)** In situ hybridization of CAGG probe to normal muscle. **(D)** In situ hybridization of CAG probe to DM1 muscle. Bar is 5 μM.

ATTCT expansion in SCA10 (*41*). The DM2 tetranucleotide and the SCA10 pentanucleotide expansions are generally longer than the expansions associated with the triplet repeat diseases, with the largest DM2 and SCA10 repeats estimated to be ≥11,000 and 4500 repeats (*41*), respectively.

Repeat instability in DM2 is complicated by the compound repeat motif $(TG)_n(TCTG)_n(CCTG)_n$ and the time-dependent somatic instability of the expansion. Although similar somatic instability is seen in DM1 and FMR1 (*42–45*), the size differences for DM2 can be much larger, up to 9000 repeats in the blood of one affected individual. Clinical anticipation has been reported in DM2/PROMM families (*46*). Although we did not observe a correlation between age of onset and expansion size, the somatic instability of the repeat (Fig. 3 and Web table 1) (*27*) complicates this and other clinical correlations between repeat length and disease.

The clinical similarities between DM1 and DM2 have helped to clarify the extensive role that RNA containing a CUG or CCUG expansion plays in DM pathogenesis. Yet, although DM1 and DM2 phenotypes are strikingly similar, they are not identical. DM2 does not show a congenital form or the severe central nervous system involvement seen in DM1. Defining the downstream differences between the CUG and CCUG expansions will be important for understanding the clinical distinctions between DM1 and DM2. Also of interest will be the identification of the mutation that causes a third type of myotonic dystrophy that has not yet been mapped to a genetic locus (*46*).

References and Notes

1. P. S. Harper, *Myotonic Dystrophy* (Saunders, London, ed. 2, 1989).
2. H. Steinert, *Dtsch. Z. Nervenheilkd.* **37**, 58 (1909).
3. C. A. Thornton, R. C. Griggs, R. T. Moxley, *Ann. Neurol.* **35**, 269 (1994).
4. K. Ricker *et al.*, *Neurology* **44**, 1448 (1994).
5. P. Groenen, B. Wieringa, *Bioessays* **20**, 901 (1998).
6. S. J. Tapscott, *Science* **289**, 1701 (2000).
7. Y.-H. Fu *et al.*, *Science* **260**, 235 (1993).
8. C. A. Boucher *et al.*, *Hum. Mol. Genet.* **4**, 1919 (1995).
9. A. D. Otten, S. J. Tapscott, *Proc. Natl. Acad. Sci. U.S.A.* **92**, 5465 (1995).
10. T. R. Klesert, A. D. Otten, T. D. Bird, S. J. Tapscott, *Nature Genet.* **16**, 402 (1997).
11. C. A. Thornton, J. P. Wymer, Z. Simmons, C. McClain, R. T. Moxley, *Nature Genet.* **16**, 407 (1997).
12. M. Alwazzan, E. Newman, M. G. Hamshere, J. D. Brook, *Hum. Mol. Genet.* **8**, 1491 (1999).
13. K. L. Taneja, M. McCurrach, M. Schalling, D. Housman, R. H. Singer, *J. Cell Biol.* **128**, 995 (1995).
14. B. M. Davis, M. E. McCurrach, K. L. Taneja, R. H. Singer, D. E. Housman, *Proc. Natl. Acad. Sci. U.S.A.* **94**, 7388 (1997).
15. L. T. Timchenko *et al.*, *Nucleic Acids Res.* **24**, 4407 (1996).
16. A. V. Philips, L. T. Timchenko, T. A. Cooper, *Science* **280**, 737 (1998).
17. X. Lu, N. A. Timchenko, L. T. Timchenko, *Hum. Mol. Genet.* **8**, 53 (1999).
18. J. W. Miller *et al.*, *EMBO J.* **19**, 4439 (2000).
19. A. Mankodi *et al.*, *Science* **289**, 1769 (2000).
20. S. Reddy *et al.*, *Nature Genet.* **13**, 325 (1996).
21. T. R. Klesert *et al.*, *Nature Genet.* **25**, 105 (2000).
22. P. S. Sarkar *et al.*, *Nature Genet.* **25**, 110 (2000).
23. L. P. W. Ranum, P. F. Rasmussen, K. A. Benzow, M. D. Koob, J. W. Day, *Nature Genet.* **19**, 196 (1998).
24. J. W. Day *et al.*, *Neuromuscular Disord.* **9**, 19 (1999).
25. We identified, obtained informed consent, performed neurological exams, and collected blood samples from DM2/PROMM family members. Genomic DNA was isolated from blood using the Puregene kit #D-5000 (Gentra Systems, Minneapolis, MN). Linkage analysis was performed using the LINKAGE package of computer programs (version 5.1) (*48*).
26. J. D. McPherson *et al.*, *Nature* **409**, 934 (2001).
27. Supplemental data are available on *Science* Online at www.sciencemag.org/cgi/content/full/293/5531/864/DC1
28. R. S. Spielman, R. E. McGinnis, W. J. Ewens, *Am. J. Hum. Genet.* **52**, 506 (1993).
29. We amplified the DM2 repeat region from genomic DNA using primers CL3N58-D F (5′-GCCTAGGGGACAAAGTGAGA-3′) and CL3N58-D R (5′-GGCCTTATAACCATGCAAATG-3′) in a PCR reaction [200 μM deoxynucleotide triphosphates (dNTPs), 10 mM tris-HCl (pH 9.0), 50 mM KCl, 0.1% Triton X-100, 0.01% (w/v) gelatin, 1 mM $MgCl_2$, 0.4 μM each primer, 0.1 U Taq] cycled 30 times (94°C for 45 s, 57°C for 45 s, 72°C for 1 min). Unrelated control DNA samples included the grandparents from the panel of 40 Centre d'Etude du Polymorphisme Humain (CEPH) families, spouses of patients diagnosed with muscular dystrophy or ataxia, and ataxia patients (n = 1360 chromosomes). Small expanded alleles were amplified from genomic DNA using primers CL3N58-B F (5′-TGAGCCGGAATCATACCAGT-3′) and CL3N58-D R in a PCR reaction [200 μM dNTPs, 50 mM Tris-HCl (pH 9.1), 14 mM $(NH_4)SO_4$, 2 mM $MgCl_2$, 0.4 μM each primer, 0.1% Tween-20, 10% dimethyl sulfoxide, 0.75 U ProofSprinter enzyme (Hybaid-AGS)] cycled 35 times (94°C for 30 s, 51°C for 30 s, 72°C for 1 min). Normal and expanded alleles amplified by PCR were cloned with the TOPO cloning kit (Invitrogen, Carlsbad, CA) and sequenced.
30. Bso BI–digested genomic DNA (5 μg) was separated on an 0.8% agarose gel, transferred to Hybond N+ membrane (Amersham, Piscataway, NJ), and hybridized with a 474-bp ZNF9 probe using Rapid-Hyb buffer (Amersham). The probe was generated by PCR using the primers probeA F (5′-GAGAACCTTGCCATTTTTCG-3′) and probeA R (5′-CACCTACAGCACTGGCAACA-3′) and random-prime-labeled (GibcoBRL, Carlsbad, CA) with ^{32}P-α-deoxyadenosine triphosphate (NEN, Boston, MA). To avoid partial digestions with Bso BI, we used 120 U of enzyme in a digestion volume of 120 μl. For more accurate sizing of the high molecular weight expansions, Eco RI–digested genomic DNA (5 μg) was separated on a 0.4% agarose gel along with high molecular weight DNA markers (Gibco-BRL).
31. L. P. W. Ranum, J. W. Day, unpublished data.
32. GenBank accession numbers are as follows: genomic sequence of the DM2 region (AF389886, AF389887); *CL3N58* sequence (AF388525); expanded *CL3N58* sequence (AF388526); ZNF9 mRNA (M28372); original ZNF9 genomic sequence (U19765); RP11-814L21 (AC022944); RP11-723o4 (AC022993); and RP11-221e20 (AC023598). The Celera accession number for the contig overlapping *ZNF9* is x2HTBKUAD8C.
33. J. C. Venter *et al.*, *Science* **291**, 1304 (2001).
34. T. B. Rajavashisth, A. K. Taylor, A. Andalibi, K. L. Svenson, A. J. Lusis, *Science* **245**, 640 (1989).
35. L. Pellizzoni, F. Lotti, B. Maras, P. Pierandrei-Amaldi, *J. Mol. Biol.* **267**, 264 (1997).
36. L. Pellizzoni, F. Lotti, S. A. Rutjes, P. Pierandrei-Amaldi, *J. Mol. Biol.* **281**, 593 (1998).
37. I. L. Flink, E. Morkin, *Gene* **163**, 279 (1995).
38. For in situ hybridization of muscle sections (13), we used 0.2 ng/μl 2′-O-methyl RNA oligos 5′ labeled with Cy3 (IDT, Coralville, IA). Fluorescence was visualized using a Zeiss Axioplan2 microscope equipped with a Spot CCD (charge-coupled device) camera (Diagnostic Instruments, Sterling Heights, MI). Appropriate exposure times were computed using the DM2/CAGG slide, and the other probes were photographed using this exposure setting.
39. N. Takahashi, N. Sasagawa, K. Suzuki, S. Ishiura, *Biochem. Biophys. Res. Commun.* **277**, 518 (2000).
40. M. D. Koob *et al.*, *Nature Genet.* **21**, 379 (1999).
41. T. Matsuura *et al.*, *Nature Genet.* **26**, 191 (2000).
42. L. J. Wong, T. Ashizawa, D. G. Monckton, C. T. Caskey, C. S. Richards, *Am. J. Hum. Genet.* **56**, 114 (1995).
43. C. Moutou, M. C. Vincent, V. Biancalana, J. L. Mandel, *Hum. Mol. Genet.* **6**, 971 (1997).
44. A. T. Helderman-van den Enden *et al.*, *J. Med. Genet.* **36**, 253 (1999).
45. A. Lopez de Munain *et al.*, *Ann. Neurol.* **35**, 374 (1994).
46. C. Schneider *et al.*, *Neurology* **55**, 383 (2000).
47. K. Ricker *et al.*, *Neurology* **52**, 170 (1999).
48. G. M. Lathrop, J. M. Lalouel, C. Julier, J. Ott, *Proc. Natl. Acad. Sci. U.S.A.* **81**, 3443 (1984).

49. We thank families and clinicians for their participation, K. Dick and L. Rasmussen for technical assistance, J. Dalton and A. Dudley for organizing family evaluations, K. Gebhard and J. Sedgwick for microphotography, M. C. Koch and D. Garcia for genetic analysis, and L. Ptacek for providing DNA from a family. Supported by the Muscle Center, Clinical Research Center, and Graduate School at the University of Minnesota; Förderverein of the Department of Neurology, University of Würzburg; Research Funds from the State of Bavaria; the Muscular Dystrophy Association, USA; and NIH grants NS35870, HG002051, and CA56266.

1 May 2001; accepted 19 June 2001